Article

A molecular dynamics investigation of the effect of pressure and orientation on the Cu consumption in Cu-Cu3Sn interface under isothermal ageing and its dissipative mechanisms during traction

Lihua Liang [1], Jicheng Zhang [1], Yangjian Xu [1], Yuanxiang Zhang [2], Wei Wang [1], and Jian Yang [3,*]

[1] College of Mechanical Engineering, Zhejiang University of Technology, Hangzhou, 310014, China; lianglihua@zjut.edu.cn (L.L.); fc_tx@163.com (J.Z.); xuyangjian@163.com (Y.X.); 752843762@qq.com (W.W.)

[2] College of Mechanical Engineering, Quzhou University, Quzhou, 324000, China; jarson_zhang@hotmail.com (Y.Z.)

[3] Institute of Process Equipment, College of Energy Engineering, Zhejiang University, Hangzhou, 310027, China

* Correspondence: zdhjkz@zju.edu.cn; Tel.: +86-571-8795-3098

Abstract: In this paper, the nanoscale dissipative mechanisms of a Cu pad in a Ball Grid Array (BGA) packaging structure during isothermal ageing and uniaxial tension were investigated by the molecular dynamics (MD) method and experiments. From the result of the isothermal ageing test, a nonuniform consumption of Cu and large amount of Kirkendall voids were observed at the interface of Cu and Cu_3Sn. To study the effect of pressure and orientation on this phenomenon, MD simulations were conducted on four types of Cu-Cu_3Sn interface structures with different orientations of Cu. By comparing the diffusion coefficients of atoms in those cases, it was found that the tensile stress would inhibit the diffusion of atoms, whereas compressive stress would accelerate it, and this would be more significant under a larger magnitude of stress and temperature. Note that, in the model with the (101) surface Cu at the interface, both Cu and Cu_3Sn have a higher diffusion coefficient compared with the model with (001) surface Cu. Thus, the orientation of Cu will also contribute to the uniform consumption of the pad. Uniaxial tension simulation combined with DXA and CSP analyses on those models also shows the model with (001) surface Cu has a greater mechanical reliability in our simulations and related experiments.

Keywords: interface structure; Molecular dynamics; diffusion coefficient; uniaxial tension; orientation

1. Introduction

To meet the requirement of portability, minimization and excellent capability, integrated circuits (ICs) have been miniaturized, and the chip integration density has grown sharply, resulting in a higher current density in the solder joint. This may cause atoms in the IC material to migrate much faster under the effect of electromigration (EM) and thermal ageing and lead to packaging failure. With the promotion of "Pb-free" solder materials, Sn-Ag-Cu (SAC) types of solder have been widely used in the electronic packaging industry. During EM and thermal ageing processes, the migration of atoms in IC materials, Cu atoms in Cu pads and Sn atoms in SAC solder joints are prone to combine together to form layer-shaped intermetallic compound (IMC), such as Cu_3Sn and Cu_6Sn_5. With the formation of these types of IMCs, Kirkendall voids and cracks usually appear around or

 doi:10.20944/preprints201801.0072.v1

within them [1]. This phenomenon mainly occurs via the large difference in diffusivity between two different grains or their components and causes atoms to migrate out of a certain region, thus leading to the formation and evolution of voids [2,3] and resulting in the degradation of mechanical strength that raises the risk of failure of electronic products. With the development of nanotechnology, nanomaterial and nanostructure [4-6] attracted people's attention, the structure and mechanical character of solder materials at a micro level have become hot issues in electronic industry.

From the research of H.W. Tseng et al. [7], spallation at the interface between Cu_3Sn and Cu was observed when at the temperature of 328 K, and a large number of Kirkendall voids appeared inside Cu_3Sn. Considering the working condition of electronic products, the reliability of Cu-Cu_3Sn interface should be taken into consideration. However, as IMC in solder material is usually at the micro-scale level, it is difficult to study its reliability via experimental methods. In recent years, the development of molecular dynamics (MD) theory has enabled micro-scale simulation of phenomena in many fields [8,9]; in particular, the diffusion rate and the mechanics behaviour of atoms can be obtained via MD simulation, which represents an alternative to experimental studies.

For the formation of Kirkendall voids in Cu_3Sn, many researchers have focused on the diffusion character of IMCs in solder joints using the MD method. Feng Gao et al. calculated and compared the self-diffusion rates of Cu and Sn in Cu_3Sn by MD simulation and verified that the large difference in diffusivity between Cu and Sn is the main cause of Kirkendall void formation within the Cu_3Sn layer in lead-free solder joints [10]. According to the results of Zequn Mei et al., most voids in Cu_3Sn are centralized near the interface with the Cu substrate [11], which cannot be explained merely by the difference between the diffusivity of Cu and Sn in Cu_3Sn. Thus, the diffusivity of atoms near the interface should be investigated separately. To address this problem, Basaran C and Sellers M S et al. studied the diffusivity of βSn in the presence of solute atoms at the grain boundary [12, 13]. According to their simulation results, the existence of solute atoms would accelerate the diffusion rate of βSn at the interface, which would make it easier to form voids. However, they only studied the grain boundary of βSn; the effects of IMC on solder diffusivity have still drawn less attention. Moreover, with the existence of a Kirkendall void, the interface strength at the Cu-Cu_3Sn interface will be reduced, thereby inducing crack formation and expansion. The propagation of such interface cracks may be accompanied by dissipative mechanisms, such as dislocation motion and structural rearrangement, which play a powerful role in the deformation process. Addressing the failure mechanism of interface structure between different grains, Pradeep Gupta et al. [14] reported the Al-$Cu_{50}Zr_{50}$ metallic glass interfacial behaviour under mode-I and mode-II loading conditions based on MD simulation and analysed the dislocation evolution during these progresses; Hsien-Chie Cheng et al. [15] and Karoon Mackenchery et al. [16] studied the mechanical character of single Cu_3Sn and Cu under tensile uniaxial tension separately. To the authors' knowledge, prior to this study, no MD simulation study reported the reliability of the Cu-Cu_3Sn interface structure. Considering the risk of this structure in electronic packaging, the investigation of the dissipative mechanisms on Cu-Cu_3Sn interface structure would facilitate evaluation of the reliability of solder joints under thermal ageing and monotonic stretching.

This paper investigated the dissipation of a Cu pad in BGA packaging structure during isothermal ageing; the results show the inhomogeneous dissipative phenomenon of Cu occurred after 350 h at a temperature of 450 K. Considering the driving force of atom diffusion during electromigration (current density, temperature, and stress) [17], the mechanical loading caused by thermal stress is the primary cause of this phenomenon. For the purpose of studying the effect of mechanical loading condition on the dissipation of Cu, this paper calculated the diffusion coefficient of atoms in perfect Cu-Cu_3Sn interface structure via MD simulation. By comparing the diffusion of atoms near the interface with different loading condition at 450 K and 600 K, the effect of both tensile stress and compressive stress on the consumption of Cu could be investigated. Moreover, the orientation of Cu was also considered to affect its diffusivity; thus, we built different interface

Preprints (www.preprints.org) | NOT PEER-REVIEWED | Posted: 9 January 2018 doi:10.20944/preprints201801.0072.v1

structures by rotating the Cu lattice to 15°, 30° and 45° along its b axis and calculated their diffusion coefficient at 450 K to investigate the effect of grain orientation to the dissipation of Cu under thermal ageing. Furthermore, the mechanical behaviour of Cu-Cu_3Sn under mode-I (normal to the interface) loading conditions is also considered here, and the study will focus on its fraction location, dissipative mechanisms, such as dislocation during deformation. This part of the study aimed at providing good predictions of the effect of Cu orientation on the interface reliability to contribute to better understanding of the dissipative mechanism in the Cu-Cu_3Sn interface structure.

2. Thermal ageing experiment on BGA structure

As is known to all, a higher current density and temperature would increase the diffusion rate of metal atoms in IC materials, thereby promoting the dissipation of the Cu pad. Hence, the isothermal ageing test is a good approach to study the effect of other factors on the dissipative of Cu. This paper conducted the isothermal ageing test with the Ball Grid Array (BGA) packaging structure, a FDMA8051L chip from Fairchild was bonded on a PCB via 6 solder joints, as shown in figure 1. The material of the solder is SAC305 (Sn-3.0Ag-0.5Cu) with a diameter of 0.3 mm. The size of PCB is 50 mm × 50 mm × 1 mm, and the whole BGA structure is only 2 mm × 2 mm × 1.07 mm, where the thick of Cu pad is 0.055 mm. Test vehicles were set in an oven at a temperature of 450 K and then were removed after a certain ageing time.

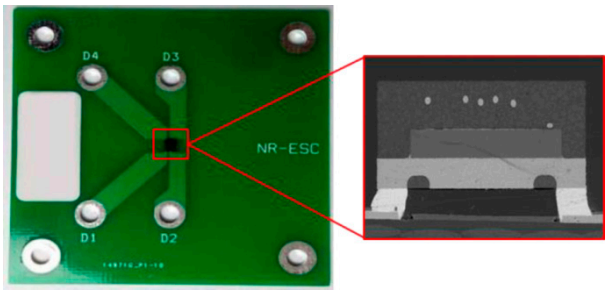

Figure 1. Details of PCB test specimen.

Figure 2 shows an SEM imaging result of a solder and pad after the ageing time of 160 h and 350 h. No significant dissipation of Cu was found in pad after ageing for 160 h, and less IMCs and Kirkendall voids were found at the interface; in contrast, figure 2 (b) shows us a completely different result: the pad was consumed heavily, and large number of IMCs are found to be distributed uniformly between the pad and the solder. With the help of EDX and EBSD analysis, the IMCs close to solder are identified as Cu_6Sn_5 and Cu_3Sn, in agreement with the results published in the literature [3,10,11]. We also find that Kirkendall voids in Cu_3Sn are mostly generated next to the Cu pad, whereas they rarely are observed in the region far away from the pad. This cannot be completely explained by comparing the diffusivity of Cu and Sn in Cu_3Sn; thus, the atom diffusivity in the Cu-Cu_3Sn interface structure should be taken into consideration.

Preprints (www.preprints.org) | NOT PEER-REVIEWED | Posted: 9 January 2018 doi:10.20944/preprints201801.0072.v1

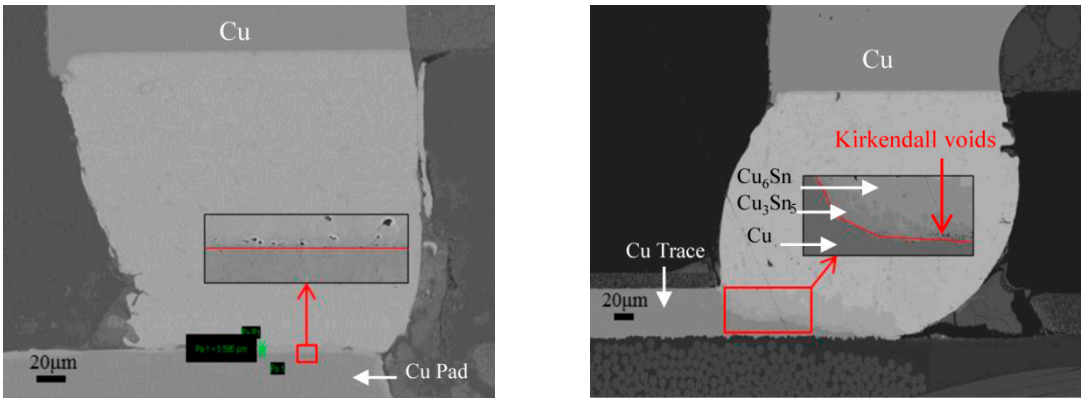

(a) (b)

Figure 2. SEM scanning results of solder and pad at 450 K after ageing: (a) 160 h and (b) 350 h

Note from figure 2 (b) that the consumption of the Cu pad shows a significant gradient character. The edge of the pad has been consumed completely, whereas the other side of the pad still has a certain amount of Cu, and the surface of the pad is shaped in the form of a slanted line. This phenomenon can be attributed to the diffusion of atoms in the trace and the pad. The Cu in the trace diffused and supplemented the drifted atoms in the pad, whereas the edge of the pad is far from the trace and obtains fewer supplements from it, resulting in Cu atoms in this region being consumed faster. In contrast, because no current loading occurred and the temperature is constant, these factors have less effect on this phenomenon. With the mechanism of thermal mismatch between different materials, a stress gradient is generated at the interface between the solder and the pad, considering the driving force of atom diffusivity in EM theory [17], stress may have its effect on this phenomenon.

To investigate the effect of stress on the dissipation of Cu atoms in the Cu-Cu_3Sn interface structure, analysis of the diffusivity of the structure under stress loading is required. One method to determine the atom diffusion rate is experimental migration rate testing [18]; however, this method requires customized samples that are monitored by scanning electron microscopy, and this method requires a quite long time to observe the movement of atoms at macro-scale. In contrast, using the MD method, the movement of atoms can be clearly observed and counted; as a result, it has become an efficient method to study material properties at the micro-scale level.

3. Molecular dynamics simulation of the dissipative mechanisms of the Cu-Cu_3Sn structure

For the atom diffusion problem, the mean square displacement (MSD) was calculated at a certain temperature in our MD simulation. MSD has been used extensively to describe the movement of atoms in solids, liquids and gases through the Einstein relations, which involves tracking atomic displacements [19]:

$$D_{\mathrm{Cu,Sn}} = \frac{1}{N_{\mathrm{Cu,Sn}}} \sum_{i=1}^{N_{\mathrm{Cu,Sn}}} \left[\lim_{t\to\infty} \frac{\mathrm{MSD}_i(t)}{6t} \right] = \frac{1}{N_{\mathrm{Cu,Sn}}} \sum_{i=1}^{N_{\mathrm{Cu,Sn}}} \left[\lim_{t\to\infty} \frac{\left\langle [\mathbf{r}_i(t) - \mathbf{r}_i(0)]^2 \right\rangle}{6t} \right] \quad (1)$$

Here, $\mathbf{r}_i(t)$ is the position of the Cu (Sn) atom i at time t; $D_{\mathrm{Cu,Sn}}$ is the diffusion coefficient, which represents the diffusivity of atoms; $N_{\mathrm{Cu,Sn}}$ is the total number of Cu and Sn atoms in the supercell; and the symbol < > denotes the average over time origins. Ideally, MSD(t) is a linear function of t after an appropriate time. Thus, linear regression is used to calculate the diffusivity from the MSD(t) curve.

Preprints (www.preprints.org) | NOT PEER-REVIEWED | Posted: 9 January 2018 doi:10.20944/preprints201801.0072.v1

The MD simulations were performed using a Large-scale Atomic/Molecular Massively Parallel Simulator (LAMMPS) [20]. To better describe the interactions between the Cu and Sn atoms, the modified embedded atom method (MEAM) interatomic potential was used. The MEAM interatomic potential has been fully discussed in references [21,22], and it has provided good results in simulating the mechanical properties [15,23], defect formation [24-26] and diffusivity [27,28] of both solid and liquid materials; thus, it will not be introduced here again.

The MEAM parameters for the pure elements of Cu and Sn were taken from the database in LAMMPS, the L12 structure is here considered as the reference structure for Cu_3Sn, and the MEAM interatomic potential of Cu-Sn used in LAMMPS can be found in [15,29], as shown in table 1. In our system, the angular screening was implemented using the method described in [22]. The value of C_{max} is 2.8 for all element combinations, and C_{min} is 0.8 for all element combinations except for a Cu atom screening two other Cu atoms, where C_{min} = 2.0 [29].

Table 1. Parameters for the MEAM potential used in LAMMPS

	Ec(eV)	r0(Å)	α	A	$\beta(0)$	$\beta(1)$	$\beta(2)$	$\beta(3)$	$t(1)$	$t(2)$	$t(3)$	ρ0	ibar
Sn	3.08	3.44	6.20	1.0	6.2	6.0	6.0	6.0	4.5	6.5	-0.183	0.7	0
Cu	3.62	2.50	5.11	1.07	3.62	2.2	6.0	2.2	3.14	2.49	2.95	1.0	0
Cu3Sn	3.50	2.68	5.38										

3.1. The effect of pressure to the diffusivity of atoms in Cu-Cu_3Sn structure

The Cu_3Sn compound is a hexagonal close-packed Cu_3Ti-type transition-metal IMC belonging to the space group 63 with Cmcm symmetry. It has been reported that the ordered Cu_3Sn is a long-period superlattice alloy with periodic antiphase domains similar to the ordered Cu_3Au [30], as shown in figure 3 (a). The interface structure built for the MD simulation is 55 Å × 64.8 Å × 63 Å of defect-free Cu layer and the same size of Cu_3Sn. The interaction between the Cu_3Sn (001) surface and the Cu (001) surface are considered in this MD simulation with no solute atoms at the interface. In this section, the simulations are performed with periodic boundary conditions in the X- and Y-directions, and non-periodic and shrink-wrapped boundary conditions are applied in the Z-direction. Before the MD simulation, the structure must be optimized. This optimization was performed in two steps. First, the two grains were placed next to each other at a distance of 3 Å; next, the structure was equilibrated using MD at the target temperature. This process is presented in figure 3 (b).

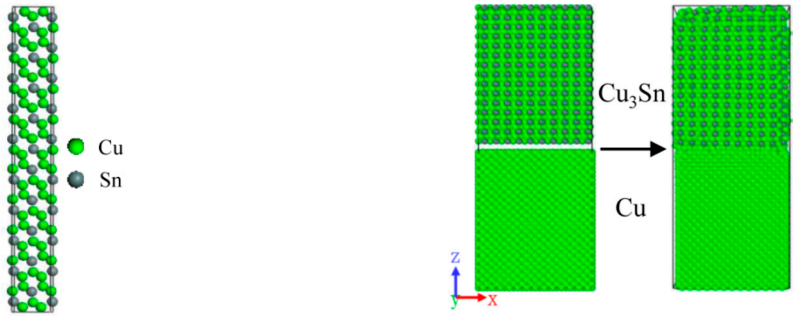

(a) (b)

Figure 3. Long-period superlattice of Cu3Sn (a) and the Cu-Cu3Sn structure (b)

Preprints (www.preprints.org) | NOT PEER-REVIEWED | Posted: 9 January 2018 doi:10.20944/preprints201801.0072.v1

According to [13], the diffusion coefficient of atoms is sensitive to their distances perpendicular to the interface; to better monitor the change of the atoms' diffusion coefficients in different areas, 8 layers were set up as surveillance regions, which were set every 6.5 Å from the interface. Each Cu region has 1344 atoms, and the Cu_3Sn region has 972 atoms. To study the effect of stress on the atom diffusivity in the structure, different pressure that perpendicular to the interface were applied on the whole model to represent the stresses that the pad suffered; a schematic diagram is shown in figure 4. Stresses of -400, -200, 200, and 400 MPa and load free (the negative sign represent for the compressive stress) were used here, and the atmosphere temperatures of 450 K and 600 K are used for comparison.

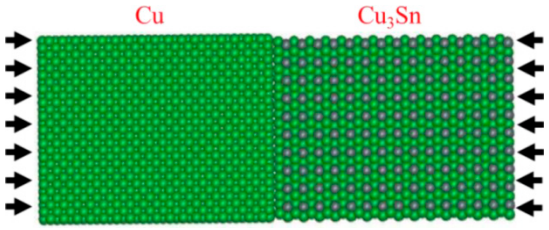

Figure 4. Molecular model with load vector

The simulation process is performed in the following manner. Structures were preheated from 100 K to the specific temperature for 30 ps under the condition of NPT (constant Number of atoms, Pressure and Temperature) with a Nose-Hoover thermostat to relax the internal stresses, and then the load vector was added gradually in the next 30 ps. Once the stress reached the given value and remained stable, the mean square displacements (MSDs) for all 8 regions in the modified structure were calculated in the following 20 ns with the time-step of 1 fs, with the data stored every 10000 time-steps (10 ps). After the simulation, the distribution of diffusion coefficient could be extracted, as shown in Figure 5.

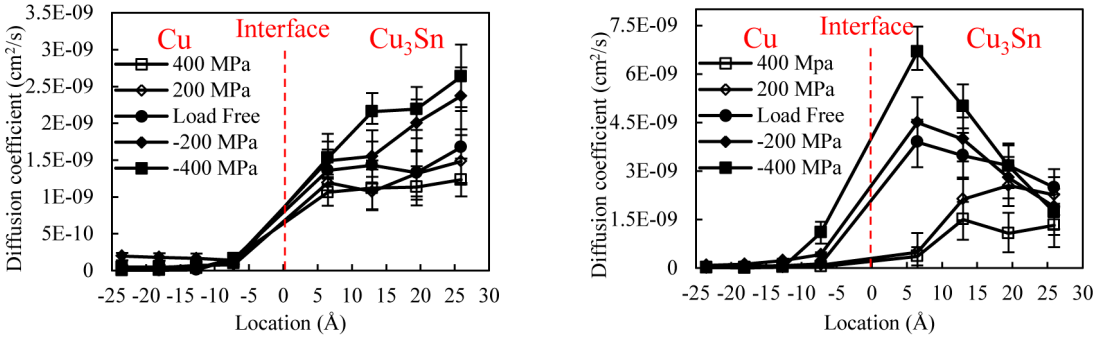

Figure 5. Diffusivity of Cu and Cu3Sn under different pressure at 450 K (a), 600 K (b)

Figures 5 (a) and (b) show that, with the change of loading condition from tensile to compression, the diffusion coefficient of Cu_3Sn rise gradually, especially for the results at 600 K. In figure 5 (b), the diffusion coefficient of Cu_3Sn nearest to the interface is 6.7E-09 cm^2/s under a compressive stress of 400 MPa, whereas, under the tensile stress of the same magnitude, it is only 3.6E-10 cm^2/s, which is much lower than the result of load free (3.9E-09 cm^2/s). This indicates the tensile stress would inhibit the diffusion of atoms in Cu_3Sn, and when the structure suffered compressive stress, atoms in Cu_3Sn would diffuse faster. Because change of the diffusion coefficient of Cu atoms in the Cu part is not so significant for both cases at 450 K, the stress has little effect on the phenomenon studied in this domain. Note that, from figure 5 (b), atoms in the Cu part nearest to the interface also have a higher diffusion coefficient (1.1E-09 cm^2/s) under a compressive stress of

Preprints (www.preprints.org) | NOT PEER-REVIEWED | Posted: 9 January 2018 doi:10.20944/preprints201801.0072.v1

400 MPa than that in load free case (1.3E-10 cm^2/s). In other words, with the increase of temperature, the effect of stress on the diffusivity of Cu part is more significant, and it has the same tendency as the atoms in Cu_3Sn. Thus, a conclusion can be made that stress will influence the diffusivity of atoms in the Cu-Cu_3Sn structure: compressive stress accelerates the diffusion of atoms near the interface whereas tensile stress inhibits it, especially for the condition of higher temperature, which is well proved by the experimental result from Chen, W. J. et al. [31]. This huge difference of atoms' diffusivity induced by different loading conditions would cause the nonuniform consumption of pad.

3.2. The effect of orientation on the diffusion character of Cu-Cu_3Sn

From the result by Yu-Jin Lia et al. [32], the orientation of Cu in pad has a great influence on the growth of Cu_3Sn that is induced by the diffusion and combination of Cu in the pad and Sn in the solder; thus, the effect of Cu orientation on the diffusivity of atoms in Cu-Cu_3Sn interface structure should not be omitted. Addressing this issue, we investigated the orientation of grains in figure 2 via EBSD technology. The distributions of grain orientation around the interface are shown in figures 6 (a) and (b).

From figures 6 (a) (b), only a 2 nm thick layer of Cu_3Sn along the interface is found when the ageing time is 160 h, and a large amount of small Cu_3Sn appeared during the consumption of the pad. From the corresponding inverse pole figures of Cu_3Sn shown in figures 6 (c) and (d), grains showed no significant preferred orientations in our test vehicles; this may be caused by the polycrystalline Cu we used in the pad. While Rui Zhang et al. [33] investigated the IMC growth with single-crystal Cu and found the orientation of Cu_3Sn was unrelated to that of Cu or Cu_6Sn_5, and single-crystal Cu would inhibit the growth of Cu_3Sn. Thus investigating the orientation of Cu in Cu-Cu_3Sn interface structure would facilitate understanding of the consumption of Cu and growth of Cu_3Sn.

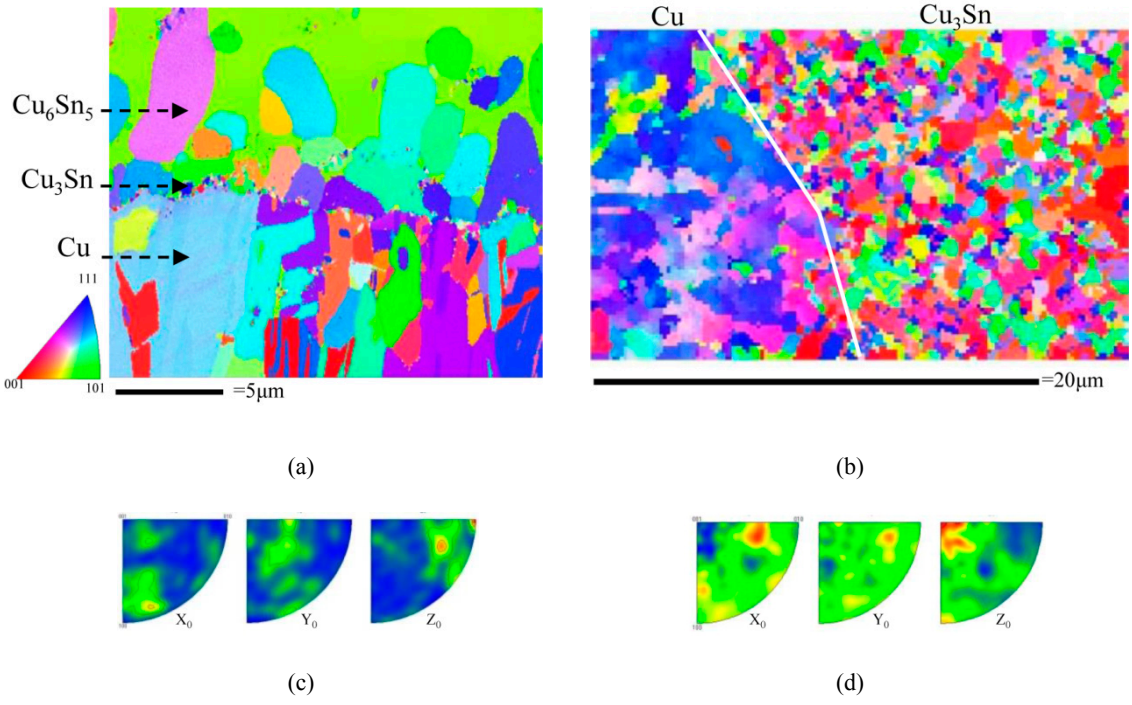

Figure 6. EBSD analysis at the interface after 160 h (a) and 350 h (b); the inverse pole figures of Cu_3Sn for 160 h (c) and 350 h (d)

Preprints (www.preprints.org) | NOT PEER-REVIEWED | Posted: 9 January 2018 doi:10.20944/preprints201801.0072.v1

The interface structure discussed in the last chapter consists of (001) surface Cu and Cu_3Sn; to investigate the effect of Cu orientation on the atomic diffusion in the structure, different interface structures with various Cu orientations are built. As Cu has a lattice structure of FCC, it is fully symmetrical in each direction; thus, the structures studied in this paper are made by rotating the a-c plane to 15°, 30°, and 45° along the b axis, as shown in figure 7. The diffusion coefficients of both regions were calculated at 450 K by the method introduced above, and then the diffusion coefficient evolution with the change of rotation angle was obtained.

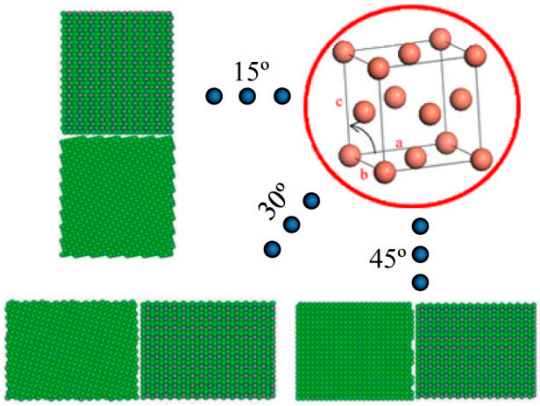

Figure 7. Three Models with different orientations of Cu

Figure 8 shows the diffusion coefficient distribution with different rotation angles at 450 K. It can be seen that, with the increase of the rotation angle, the diffusion coefficient of Cu_3Sn rises gradually and reaches a highest magnitude when the rotation angle is 45°. Compared to the result that the structure of (001) surface Cu (1.36E-09 cm^2/s), the diffusion coefficient of Cu_3Sn in the structure of (101) surface Cu combined with the Cu_3Sn increases to 2.95E-09 cm^2/s. Moreover, the diffusion coefficients of the Cu layers in rotated structure also have a higher magnitude than that in the structure of (001) surface Cu, with the highest magnitude in the structure of rotation angle of 30°. The higher diffusion coefficient indicates that atoms will be more active, thereby accelerating the consumption and growth of Cu and Cu_3Sn, respectively, and in the structure of (101) surface Cu (rotation angle is 45°) combined with the Cu_3Sn, the large difference of diffusion coefficient between Cu and Cu_3Sn near the interface will promote the formation of Kirkendall voids, thereby decreasing the reliability of the solder structure, which in turn reduces the packaging lifetime.

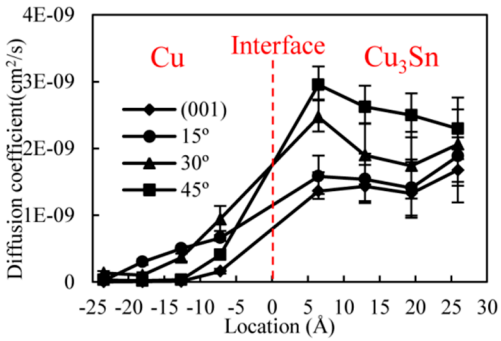

Figure 8. The effect of Cu orientation to Diffusivity of Cu and Cu3Sn at 450 K

Preprints (www.preprints.org) | NOT PEER-REVIEWED | Posted: 9 January 2018 doi:10.20944/preprints201801.0072.v1

3.3. Dissipative mechanism analysis of Cu-Cu_3Sn under mode-I loading condition

3.3.1. Mechanical behaviour of Cu-Cu_3Sn with different orientation of Cu

With the consumption of the Cu pad and the appearance of Kirkendall voids in Cu_3Sn, crack expansion is prone to occur along the Cu-Cu_3Sn interface, causing slabbing to occur between Cu and Cu_3Sn. A well-known method to estimate the interface reliability is the cohesive zone method (CZM), In this method, large deformations and interatomic separation is based on the concept of the crack tip cohesive zone [34,35]. Cohesive zone models are the popular models for modelling interface fracture. In the CZM, the relationship between traction and separation should be obtained and used for the measurement of interface strength. The traction-separation relationship is parameterized through empirical data or by the method of inversion to obtain the parameters from the tensile test. Based on this approach, some researchers extracted the traction-displacement curve from MD simulation and used it to estimate the cohesive strength of different interface structures.

From the results discussed above, the orientation of Cu directly affected the diffusivity of atoms in the Cu-Cu_3Sn interface structure. To study its effect on the interface strength of Cu-Cu_3Sn, this paper investigated the mechanical behaviour of the structures under mode-I loading condition, and the relationship between averaged stress along the traction direction and displacement during deformation is used here to compare the interface strength of different models.

In this part of simulation, an asymmetric boundary condition is applied in each direction. The structure was preheated to 450 K under the condition of NVT, and then 21 Å for both sides of Cu and Cu_3Sn were set as rigid bodies, as shown in figure 9 (a); to deform the interface model under mode-I, uniform velocity with a strain rate of 0.0027 ps^{-1} is applied to the rigid region of Cu_3Sn along the direction that perpendicular to the interface. Virial stress is used for calculation of the tensile stress at the atomic level [36,37], as can be expressed as follows:

$$S_{\alpha\beta} = -\sum_i m_i v_\beta^\alpha + \frac{1}{2}\sum_i \sum_{j \neq i} F_{ij}^\alpha r_{ij}^\beta \quad (2)$$

where m_i and v_i are the mass and velocity, respectively, of the atom i, F_{ij} is the force between atom i and j, r_{ij} is the distance between atoms i and j, and the indices α and β denote the Cartesian components. The virial stress will be exported every 1 ps, and the averaged stress-displacement results for different model are shown in figure 9 (b).

From figure 9 (b), it can be found that the extension of the interface model begins with an elastic deformation, and after the curve reaches the first peak stress, it would drop sharply. Note that the model of the (001) surface only has one yield point, and the curve of averaged tress-displacement is shaped similar to the bilinear cohesive zone model; others have at least two or more yield points during deformation. In other words, the model of the (001) surface shows the strong brittleness, and with the increase of rotation angles for Cu lattice, the structure presents more toughness. Moreover, the mechanical responses for different structures vary from one another. the structure with (001) surface Cu has a yield stress of 9573 MPa, which is much larger than the results obtained from other structures (range of 5300-6400 MPa) and is slightly lower than the tensile result for single Cu_3Sn from Hsien-Chie Cheng et al. [15] (σ_{22} with the strain rate of 0.362% ps^{-1} in their simulation).

Preprints (www.preprints.org) | NOT PEER-REVIEWED | Posted: 9 January 2018 doi:10.20944/preprints201801.0072.v1

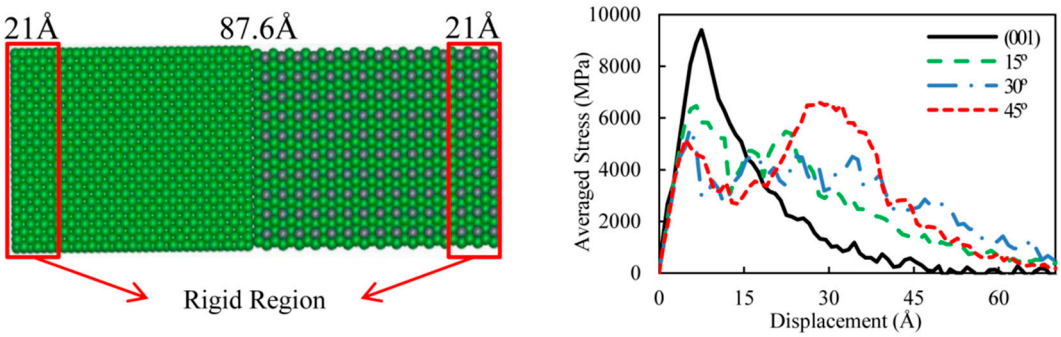

(a) (b)

Figure 9. Schematic boundary of traction model (a); averaged stress-displacement curve for different models (b)

From the atomic position snapshots of all interface models after failure exported in figure 10, it is obvious that there are two types of fraction locations in different models. The fracture in the (001) surface model is located at the interface; thus, the stress obtained here is mainly accumulated by the interface separation, whereas with increasing rotation angle, fracture locations move towards the Cu part gradually, thereby the lower yield stress of Cu induces the decrease of stress during traction in figure 9 (b). This indicated the orientation of Cu influences the fraction location in Cu-Cu_3Sn interface structure and then affects its interface strength, and the structure of the combination of the (001) surface Cu and Cu_3Sn has the highest interface strength.

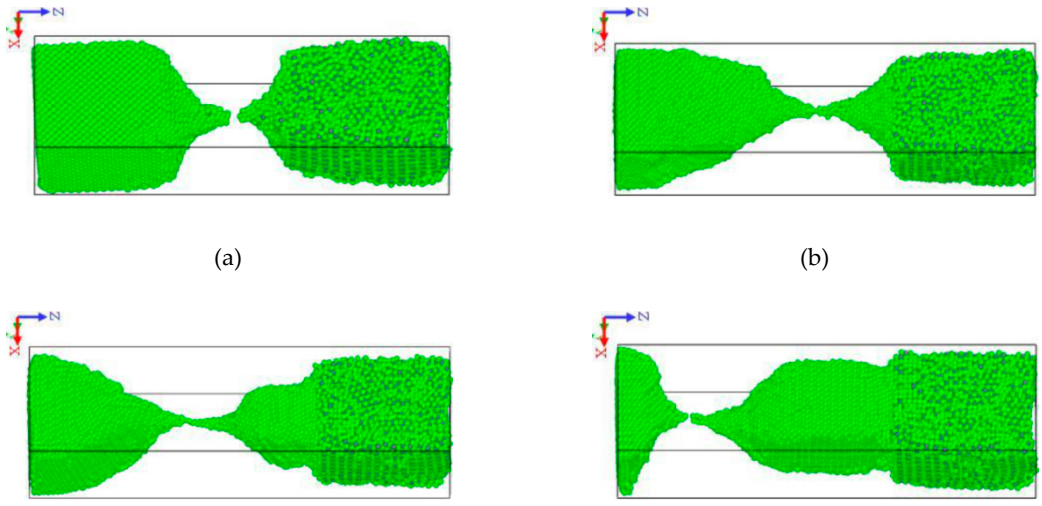

(a) (b)

(c) (d)

Figure 10. Fraction location of different model after deforming: (001) surface (a), 15° (b), 30° (c), and 45° (d)

Preprints (www.preprints.org) | NOT PEER-REVIEWED | Posted: 9 January 2018 doi:10.20944/preprints201801.0072.v1

3.3.2. CSP and DXA analysis during deformation

For visualization of the defects (dislocations, stacking faults, and nanotwins, etc.) during deformation, the centro-symmetry parameter (CSP) introduced by Kelchner et al. [38] will be used here. The CSP for a given atom is defined as follows:

$$\mathrm{CSP} = \sum_{i=1}^{N/2} \left| \boldsymbol{R}_i - \boldsymbol{R}_{i+N/2} \right| \tag{3}$$

where N is the number of nearest neighbours (as Cu has the FCC structure, N = 12) for the underlying lattice of atoms. $\boldsymbol{R}_i$ and $\boldsymbol{R}_{i+N/2}$ are vectors corresponding to the particular pairs of opposite nearest neighbours to the central atom. For a perfect lattice, the value of CSP is zero, whereas, for the regions that have defects or atoms close to free surfaces, it will increase to a positive value; a large CSP value indicates the symmetry is broken. We used OVITO software [39] for CSP analysis and the dislocation extraction algorithm, DXA (Dislocation analysis module in the software), to visualize the extracted dislocations and the corresponding Burgers vectors, which are observed as lines.

Considering the asymmetry of Cu_3Sn, it is difficult to evaluate its defect via CSP and DXA. From the atomic position snapshots in figure 10, Cu is the crucial part during the deformation; thus, the investigation of defects in the Cu part will be helpful to understand the difference between the deformation process of different models.

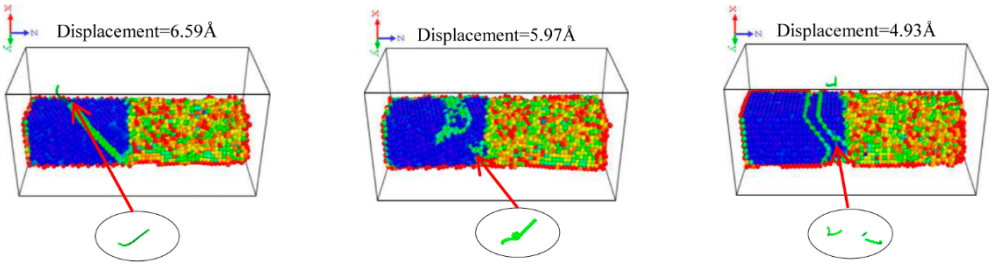

Figure 11. CSP and DXA snapshot corresponding to the first peak stress for the model with rotation angle of 15° (a), 30° (b), and 45° (c)

Figure 11 shows us the CSP and DXA snapshot corresponding to the first peak stress for both three interface models. It should be noted that the dislocation cores nucleate at the interface for all models; the DXA analysis results in the circle also shows all Shockley partials having Burgers vector 1/6 [112], and from figure 11 (c) we can find the maximum stress of the interface could be attributed to the nucleation of parallel stacking faults. It is worth noting that the extensions of these dislocations differ with each other: in the model with the Cu lattice rotates 15°, the dislocation core nucleates at the edge of the surface and extends inside the Cu part; when it rotates 30°, dislocation cores nucleate both at the interface and in the middle of the Cu region and have a tendency to combine together, resulting in fracture occurring in the middle of Cu; in the model that rotates 45°, a significant slip along the (001) surface of Cu is observed, and these defects will transfer apart from the interface to the bottom. This distinguishing of dislocations may lead to the difference in the fracture location between different models.

 doi:10.20944/preprints201801.0072.v1

4. Conclusions

This paper involved the isothermal ageing test with the BGA packaging structure at 450 K. Using the SEM and EBSD techniques, a nonuniform consumption of the Cu pad was observed, with a significant gradient along the solder interface. Considering the pad suffered a stress gradient in our test sample, and a large number of Kirkendall voids appeared at the interface between the Cu pad and the Cu_3Sn type of IMC. Because pressure was considered as the cause of this phenomenon, this paper investigated the effect of stress on atom diffusivity in Cu-Cu_3Sn interface structure via MD simulation. By comparing the diffusion coefficient of each region in the structure with various magnitude of stress, tensile stress was found to inhibit the diffusion of atoms in Cu_3Sn, whereas the compress stress promotes it; this difference becomes more significant with a larger magnitude of stress. In our simulation at both 450 K and 600 K, the diffusion coefficients of Cu_3Sn are much higher than it in Cu part, especially for the condition at 600 K, the diffusion coefficient of Cu_3Sn nearest to the interface is 6.7E-09 cm^2/s under a compressive stress of 400 MPa, which is 18.6 times larger than the result under the tensile stress of the same magnitude (3.6E-10 cm^2/s). Moreover, at the temperature of 600 K, the same phenomenon could also be found in the Cu part, with a nearly 10-fold difference of diffusion coefficient between the result under a compress stress of 400 MPa and loadfree case. This large difference of diffusion coefficient will surely induce the uniform consumption of the pad.

This paper also investigated the effect of Cu orientation on the diffusivity of atoms in Cu-Cu_3Sn interface structure. From the distribution of diffusion coefficient in four types of structures at 450 K, we can find that, the diffusion coefficient of Cu_3Sn in the model that has (101) surface Cu at the interface has the highest magnitude when compared with other models: Compared to the result in the structure with the (001) surface Cu, the diffusion coefficient of Cu_3Sn in the structure that (101) surface Cu increased to 2.95E-09 cm^2/s, and the diffusion coefficients of Cu layers in both rotated structures have a higher magnitude than that in the structure with (001) surface Cu. Thus, the orientation of Cu has a higher effect on the uniform consumption of pad compared to the stress at 450 K, and a single-crystal Cu pad with the (001) plane at the solder interface will be of great help to reduce the consumption of Cu.

To evaluate the interface strength of the Cu-Cu3Sn interface structure, a tensile test perpendicular to the interface for both structures with different orientations of Cu was simulated in this paper. The result showed the model of (001) surface has strong brittleness, and it has the largest interface strength of 9573 MPa. With increase of rotation angles for the Cu lattice, the structure shows more toughness, and the interface strength is reduced to a range of 5300-6400 MPa. From the atomic position snapshots, the fraction locations are responsible for the difference of interface strength, and the fracture in the (001) surface model is located at the interface, whereas, with the increase of rotation angle, the fracture locations move towards the Cu part gradually. This means the interface strength in Cu-Cu3Sn interface structure is greater than the yield stress of the related single crystal Cu, so the orientation of Cu in pad will be the critical factor of the reliability in Cu-Cu3Sn interface structure. Combined with the CSP and DXA results, dislocation cores appeared at the interface first, and only Shockley partials that have Burgers vector 1/6 [112] could be found in our simulation, and the maximum stress of the interface is attributed to the nucleation of parallel stacking faults. The extensions of dislocation in different models differ from one another with the

change of rotation angle, and this induces the change of fraction location and interface strength. Combined with the diffusion analysis on the model built in this paper, we verified the structure with the Cu_3Sn-(001) Cu has a greater mechanical reliability.

Acknowledgments: This work was supported by the National Natural Science Foundation of China (Nos. 51375447, 51375444 ,51375448, 51605252).

Author Contributions: For research articles with several authors, a short paragraph specifying their individual contributions must be provided. The following statements should be used "X.X. and Y.Y. conceived and designed the experiments; X.X. performed the experiments; X.X. and Y.Y. analyzed the data; W.W. contributed reagents/materials/analysis tools; Y.Y. wrote the paper." Authorship must be limited to those who have contributed substantially to the work reported.

Conflicts of Interest: The authors declare no conflict of interest.

References

1. Lai, Y.S.; Chiu, Y.T.; Chen, J. Electromigration reliability and morphologies of Cu pillar flip-chip solder joints with Cu substrate pad metallization. Journal of Electronic Materials, 2008, 37(10), 1624-1630.
2. K. Zeng; K.N. Tu. Six cases of reliability study of pb-free solder joints in electronic packaging technology. Materials Science and Engineering: R: Reports, 2002, 38(2), 55-105.
3. Borgesen, P; Yin, L.; Kondos, P. Assessing the risk of "kirkendall voiding" in Cu3Sn. Microelectronics Reliability, 2011, 51(4), 837-846.
4. Tseng, H.W.; Lu, C.T.; Hsiao, Y.H.; Liao, P.L.; Chuang, Y.C.; Chung, T.Y.; Liu, C.Y.; Electromigration induced failures at Cu/Sn/Cu flip-chip joint interfaces. Microelectronics Reliability, 2010, 50(8), 1159-1162.
5. Wu, H.; Zhu, K.; Cao, B.; Zhang, Z.; Wu, B.; Liang, L.; Chai G.; Liu, A. Smart design of wettability-patterned gradients on substrate-independent coated surfaces to control unidirectional spreading of droplets. Soft Matter, 2017, 13(16), 2995-3002.
6. Wu, H.; Zhu, K.; Wu, B.; Lou, J.; Zhang, Z.; Chai, G. Influence of structured sidewalls on the wetting states and superhydrophobic stability of surfaces with dual-scale roughness. Applied Surface Science, 2016, 382, 111-120.
7. Wu, H., Yang, Z., Cao, B., Zhang, Z., Zhu, K., Wu, B., Jiang, S.; Chai, G. Wetting and Dewetting Transitions on Submerged Superhydrophobic Surfaces with Hierarchical Structures. Langmuir, 2016, 33(1), 407-416.
8. Cao, W.; Tow, G.M.; Lu, L.; Huang, L.; Lu, X. Diffusion of CO2/CH4 confined in narrow carbon nanotube bundles. Molecular Physics, 2016, 114(16-17), 2530-2540.
9. Ruberto, R.; Pastore, G.; Akdeniz, Z.; Tosi, M.P. Structure and diffusion in aluminium and gallium trihalide melts from simulations based on intramolecular force laws. Molecular Physics, 2007, 105(17-18), 2383-2392.Fantini, D.; Zanetti, M.; Costa, L. Polystyrene Microspheres and Nanospheres Produced by Electrospray. Macromol. Rapid Commun. 2006, 27, 2038–2042.
10. Gao, F.; Qu, J. Calculating the diffusivity of Cu and Sn in Cu3Sn intermetallic by molecular dynamics simulations. Materials Letters, 2012, 73, 92-94.
11. Mei, Z.; Ahmad, M.; Hu, M.; Ramakrishna, G. Kirkendall voids at Cu/solder interface and their effects on solder joint reliability. In Electronic Components and Technology Conference, Proceedings, 55th, IEEE, Lake Buena Vista, FL, USA, 2005, 415-420.
12. Basaran, C.; Sellers, M.S.; Schultz, A.J.; Kofke, D.A.; Lee, Y. Solder joint grain boundary structure and diffusivity via molecular dynamics simulations. In Thermal and Thermomechanical Phenomena in Electronic Systems (ITherm), 2012 13th IEEE Intersociety Conference on . IEEE, San Diego, CA, USA, 2012: 514-517

13. Sellers, M.S.; Schultz, A.J.; Basaran, C.; Kofke, D.A. Effect of Cu and Ag solute segregation on β Sn grain boundary diffusivity. Journal of Applied Physics, 2011, 110(1), 013528.

14. Gupta, P.; Pal, S.; Yedla, N. Molecular dynamics based cohesive zone modeling of Al (metal)–Cu 50 Zr 50 (metallic glass) interfacial mechanical behavior and investigation of dissipative mechanisms. Materials & Design, 2016, 105, 41-50.

15. Cheng, H.C.; Yu, C.F.; Chen, W.H. Strain-and strain-rate-dependent mechanical properties and behaviors of Cu3Sn compound using molecular dynamics simulation. Journal of Materials Science, 2012, 47(7), 3103-3114.

16. Mackenchery, K.; Valisetty, R.R.; Namburu, R.R.; Stukowski, A.; Rajendran, A.M.; Dongare, A. M. Dislocation evolution and peak spall strengths in single crystal and nanocrystalline Cu. Journal of Applied Physics, 2016, 119(4), 044301.

17. Tan, Cher Ming, and Arijit Roy. "Electromigration in ULSI interconnects." Materials Science and Engineering: R: Reports, 2007, 58(1): 1-75

18. Wu F.S; Wang L.; Wu Y.P; Zhang J.S; Jiang Y.Q. Test Methods for Electromigration in IC Interconnects and Their Evaluations. Microelectronics, 2004, 34(5): 489-492.

19. Frenkel, D.; Smit, B. Understanding Molecular Simulation: From Algorithms to Applications. Academic Press, 1996, Inc.

20. Plimpton, S. Fast parallel algorithms for short-range molecular dynamics. Journal of Computational Physics, 1995, 117(1), 1-19.

21. Baskes, M.I. Modified embedded-atom potentials for cubic materials and impurities. Physical Review B, 1992, 46(5), 2727.

22. Baskes, M.I.; Angelo, J.E.; Bisson, C.L. Atomistic calculations of composite interfaces. Modelling and Simulation in Materials Science and Engineering, 1994, 2(3A), 505.

23. Cherne, F.J.; Baskes, M.I; Deymier, P.A. Properties of liquid nickel: A critical comparison of EAM and MEAM calculations. Physical Review B, 2001, 65(2), 853-857.

24. Edström, D.; Sangiovanni, D.G; Hultman, L.; Chirita, V.; Petrov, I.; Greene J.E. Ti and n adatom descent pathways to the terrace from atop two-dimensional tin/tin(001) islands. Thin Solid Films, 2014, 558(17), 37-46.

25. Zhang, L.; Lu, C.; Pei, L.; Zhao, X.; Zhang, J.; Tieu, K. Evaluation of Mechanical Properties of Σ5 (210)/[001] Tilt Grain Boundary with Self-Interstitial Atoms by Molecular Dynamics Simulation. Journal of Nanomaterials, 2017.

26. Li, Q.; Huang, C.; Liang, Y.; Fu, T.; Peng, T. Molecular Dynamics Simulation of Nanoindentation of Cu/Au Thin Films at Different Temperatures. Journal of Nanomaterials, 2016.

27. Timmerscheidt, T.A.; Appen, J.V.; Dronskowski, R.A molecular-dynamics study on carbon diffusion in face-centered cubic iron.Computational Materials Science, 2014,91(2), 235-239.

28. Lee, B. M.; Lee, B. J. A comparative study on hydrogen diffusion in amorphous and crystalline metals using a molecular dynamics simulation. Metallurgical & Materials Transactions A, 2014,45(6), 2906-2915.

29. Aguilar, J.F.; Ravelo, R.; Baskes, M.I. Morphology and dynamics of 2D Sn-Cu alloys on (100) and (111) Cu surfaces. Modelling & Simulation in Materials Science & Engineering, 2000,8(3), 335.

30. Y. Watanabe; Y. Fujinaga; H. Iwasaki. Lattice modulation in the long-period superstructure of Cu3Sn. Acta Crystallographica. Section B, Structural Science, 1983,39(3), 306-311.

31. Chen, W.J.; Lee, Y.L.; Wu, T.Y.; Chen, T.C.; Hsu, C.H.; Lin, M.T. Effects of electrical current and external stress on the electromigration of intermetallic compounds between the flip-chip solder and copper substrate. Journal of Electronic Materials,2017, (12), 1-14.

32. Li, Y.J.; Chen, C. Growth of Cu6Sn5 and Cu3Sn intermetallic compounds on (111)-, (100)-, and randomly-oriented copper films. Microsystems, Packaging, Assembly and Circuits Technology Conference, IEEE, Taipei, Taiwan, 2016, 42-44.

33. Zhang, R.; Tian, Y.; Hang, C.; Liu, B.; Wang, C. Formation mechanism and orientation of Cu3Sn grains in Cu–Sn intermetallic compound joints. Materials Letters, 2013,110(11), 137-140.

34. Dugdale, D.S. Yielding of steel sheets containing slits. Journal of the Mechanics & Physics of Solids, 1960,8(2), 100-104.

35. Barenblatt, G.I. The mathematical theory of equilibrium cracks in brittle fracture. Advances in Applied Mechanics, 1962,7, 55-129.

36. Dandekar, C.R.; Shin, Y.C. Molecular dynamics based cohesive zone law for describing al–sic interface mechanics. Composites Part A, 2011,42(4), 355-363.

37. Spearot, D.E.; Jacob, K.I.; Mcdowell, D.L. Non-local separation constitutive laws for interfaces and their relation to nanoscale simulations. Mechanics of Materials, 2004,36(9), 825-847.

38. Kelchner, C.L.; Plimpton, S.J.; Hamilton, J.C. Dislocation nucleation and defect structure during surface indentation. Physical Review B, 2011,58(17), 11085-11088.

39. Stukowski, A. Visualization and analysis of atomistic simulation data with ovito-the open visualization tool. Modelling Simul.mater.sci.eng, 2009,18(6), 2154-2162.